Insights into the monolayer formation on WO_3/TiO_2 catalyst for glycerol dehydration to acrolein

Martina Battisti,[a,b] Nico Hollik,[b] Ansgar Meise,[c] Marc Heggen,[c] Chalachew Mebrahtu,[a,b] Regina Palkovits*[a,b]

a. Institute for a Sustainable Hydrogen Economy, Forschungszentrum Jülich GmbH, 52428 Jülich, Germany. E-mail: r.palkovits@fz-juelich.de

b. Chair of Heterogeneous Catalysis and Technical Chemistry, Institute for Technical and Macromolecular Chemistry, RWTH Aachen University, 52074 Aachen, Germany. E-mail: palkovits@itmc.rwth-aachen.de

c. Ernst Ruska-Centre for Microscopy and Spectroscopy with Electrons, Forschungszentrum Jülich, Jülich, Germany

Table of Contents

1. Catalytic activity

Conversion and selectivity were calculated based on the following equations and are reported in Figure S1, Table S1, Table S2, Figure S2, and Table S3.

$$X_{Glycerol}(\%) = \frac{n^{0}_{Glycerol} - n_{Glycerol}}{n^{0}_{Glycerol}} \cdot 100$$

$$S_{Product}(\%) = \frac{n_{Product}}{n^{0}_{Glycerol} - n_{Glycerol}} \cdot 100$$

$X_{Glycerol}(\%)$ = Glycerol conversion
$n^{0}_{Glycerol}$ = Glycerol moles in the feed stream
$n_{Glycerol}$ = Glycerol moles in the outlet stream
$S_{Product}(\%)$ = Product selectivity
$n_{Product}$ = Product moles in the outlet stream

The average carbon balance during the experiments was calculated from the following equation, and the values can be found in Table S1 and Table S3:

$$C(\%) = \left(\frac{\sum \frac{X_{Glycerol}(\%)}{100} \cdot \frac{S_{Product}(\%)}{100} \cdot n_C + \left(1 - \frac{X_{Glycerol}(\%)}{100}\right) \cdot n_{GLY}}{n_{GLY}} \right) \cdot 100$$

$C(\%)$ = Carbon balance
n_C = Number of carbons in one molecule of the product considered
n_{GLY} = Number of carbons in one molecule of glycerol = 3

The catalytic activity data reported in Figures S1-S2 and Tables S1-S3 are limited to the main products formed during the reaction (Selectivity > 1%), which are considered in this study. Other products were observed in trace amounts but not quantified and reported, such as allyl alcohol, propionaldehyde, propionic acid and cyclic acetals of glycerol. Additionally, CO and CO_2 were present in the gaseous outlet of the reactor but not quantified. We can hypothesize that the carbon loss during the reaction derives both from the formation of CO and CO_2 and from the formation of heavy carbonaceous deposits on the catalyst and in the reactor, which were observed

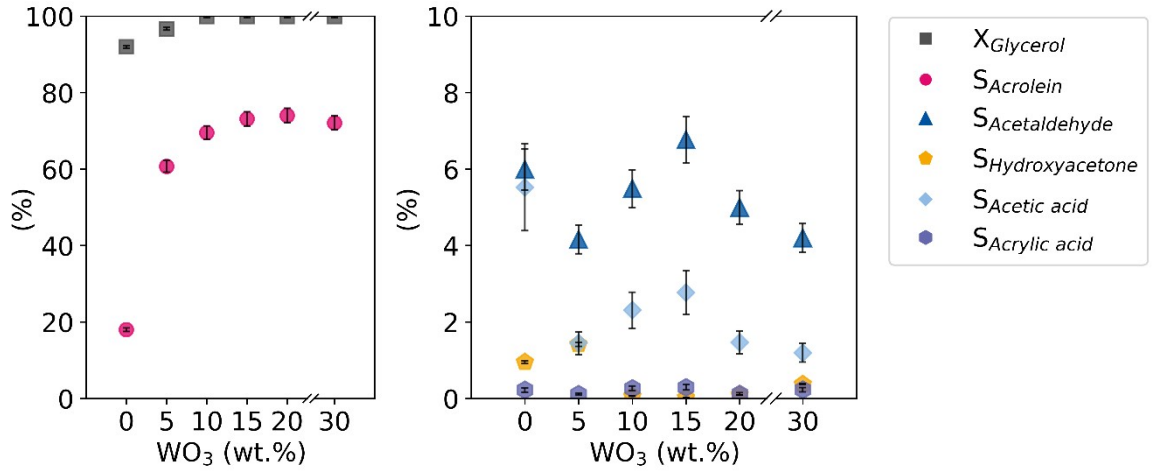

after reaction.

Figure S1. Glycerol conversion and acrolein selectivity (right) and by-products selectivity (left) for the WO_3/TiO_2 catalysts with increasing WO_3 loading. Reaction conditions: T = 280 °C, contact time = 0.36 s, HSV 15,000 mL h^{-1} g^{-1}, 4.1 vol% Glycerol, 83.6 vol% H_2O, 2.5 vol% O_2, 9.8 vol% N_2.

W loading (wt.%)	X_GLY (%)	S_ACR (%)	S_ACH (%)	S_HXY (%)	S_ACA (%)	S_AYA (%)	C (%)
0	91.96	17.98	5.99	0.95	5.52	0.22	-
5	96.65	60.71	4.16	1.41	1.45	0.11	67.1
10	99.86	69.54	5.48	0.060	2.31	0.26	75.1
15	99.86	73.13	6.77	0.019	2.77	0.29	79.8
20	99.86	74.02	4.99	0.088	1.46	0.12	78.6
30	99.86	72.06	4.20	0.37	1.19	0.23	76.3

Table S1. Glycerol conversion, products selectivity and carbon balance for the data reported in Figure S1.

GLY=Glycerol, ACR=Acrolein, ACH=Acetaldehyde, HXY=Hydroxyacetone, ACA=Acetic acid, AYA=Acrylic acid, C=Carbon balance

Table S2. Standard error for the glycerol conversion and products selectivity values relative to table S1 and reported in Figure S1.

W loading (wt.%)	Std.Err. X_GLY (%) [a]	Std.Err. S_ACR (%)	Std.Err. S_ACH (%)	Std.Err. S_HXY (%)	Std.Err. S_ACA (%)	Std.Err. S_AYA (%)
0	0.33	0.46	0.53	0.04	1.13	0.06
5	0.33	1.55	0.37	0.05	0.30	0.03
10	0.33	1.78	0.49	0.002	0.47	0.07
15	0.33	1.87	0.60	0.001	0.57	0.07
20	0.33	1.89	0.45	0.003	0.30	0.03
30	0.33	1.84	0.37	0.01	0.24	0.06

GLY=Glycerol, ACR=Acrolein, ACH=Acetaldehyde, HXY=Hydroxyacetone, ACA=Acetic acid, AYA=Acrylic acid; [a] The standard error of glycerol was calculated from the detection limit, since it was not detected in any of the reactions.

The 15 and 20 wt.% WO_3/TiO_2 were compared at higher space velocity to assess the intrinsic activity of the catalyst. Due to the lower conversion, the quantification of the high amount of unconverted glycerol was not possible via gas chromatography. Thus, the unreacted glycerol was quantified with a Shimadzu HPLC system 2020 equipped with a Refractive Index Detector (RID-10A). The device mounted 3 linear coupled columns packed with organic resins from CS (30 x 8 mm, 100 x 8 mm, 250 x 8 mm). The liquid phase was a 2 mM trifluoroacetic acid aqueous solution, with a total flow of 2 mL min^{-1}. The oven temperature was set to 40°C, with a 25 min runtime per sample.

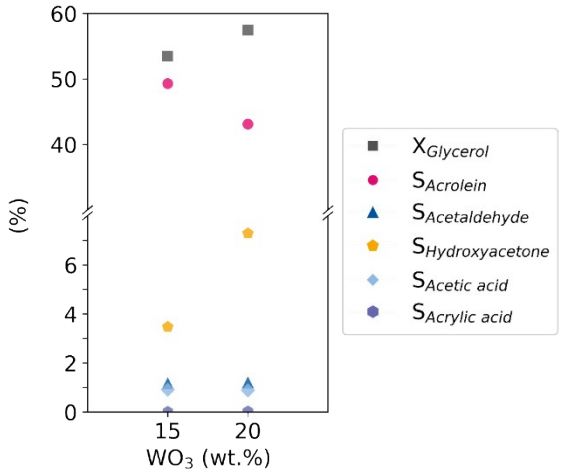

Figure S2. Comparison of the glycerol conversion and products selectivity for the 15 and 20 wt.% WO_3/TiO_2 catalysts. Reaction conditions: T = 280 °C, contact time = 0.36 s, HSV 120,000 mL h^{-1} g^{-1}, 4.1 vol% Glycerol, 83.6 vol% H_2O, 2.5 vol% O_2, 9.8 vol% N_2.

Table S3. Glycerol conversion, products selectivity and carbon balance for the data reported in Figure S2.

W loading (wt.%)	X_GLY_HPLC (%)	S_ACR (%)	S_ACH (%)	S_HXY (%)	S_ACA (%)	S_AYA (%)	C (%)
15	53.5	49.3	1.2	3.5	0.91	-	75.5
20	57.4	43.1	1.2	7.3	0.89	-	72.3

GLY=Glycerol, ACR=Acrolein, ACH=Acetaldehyde, HXY=Hydroxyacetone, ACA=Acetic acid, AYA=Acrylic acid, C=Carbon balance

2. N_2-Physisorption

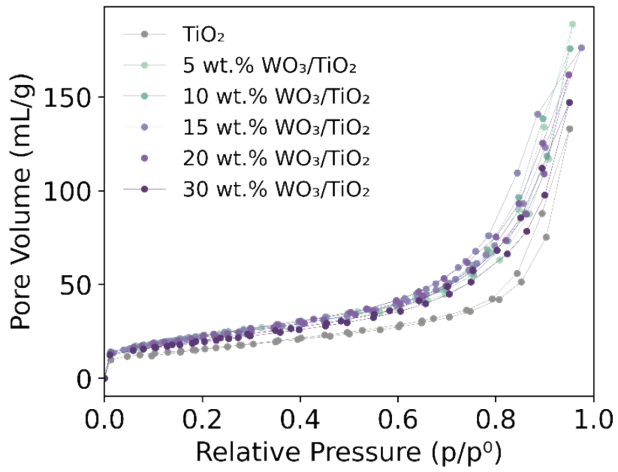

Figure S3. Nitrogen physisorption isotherms for the WO_3/TiO_2 catalysts.

3. Calculated W surface density

$$\text{Calculated W Surface Density} = \frac{\frac{WO_3\ \text{wt.\%}}{100} N_A}{MM_{WO_3} SSA_{TiO_2} \left(1 - \frac{WO_3\ \text{wt.\%}}{100}\right)}$$

$WO_3\ \text{wt.\%}$ = WO_3 weight percent as measured via ICP-OES

N_A = Avogadro constant

MM_{WO_3}= Molar Mass WO_3

SSA_{TiO_2} = Specific Surface Area of the TiO_2 support (105 $m^2\ g^{-1}$)

4. NH_3 TPD – Total acidity of the catalyst

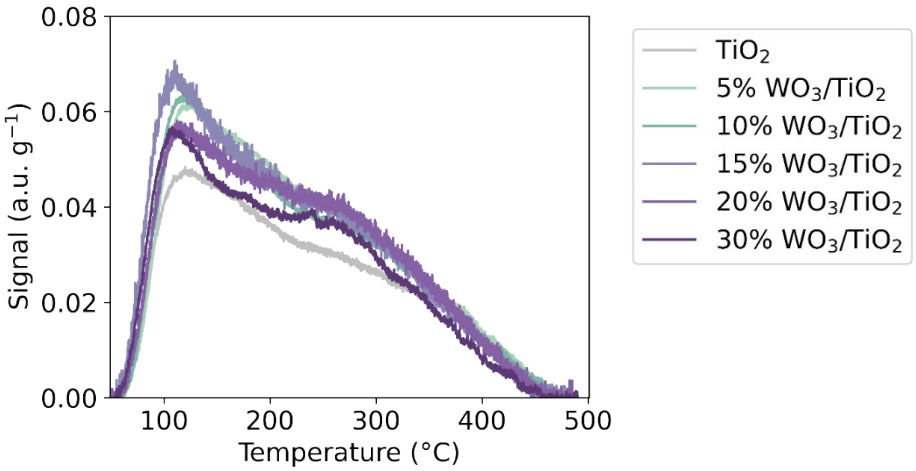

Figure S4. Ammonia TPD profiles for the for the WO_3/TiO_2 catalysts.

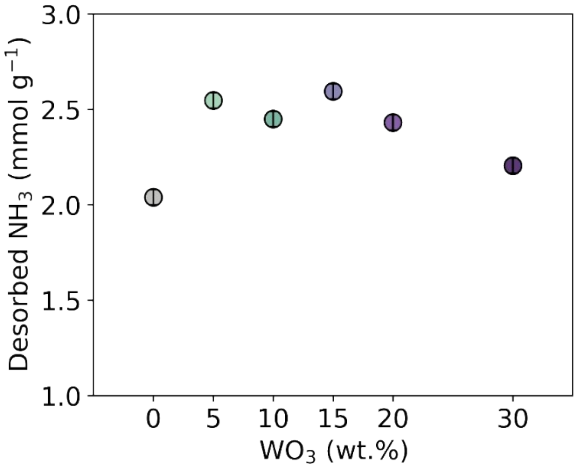

Figure S5. Calculated desorbed ammonia from the NH_3-TPD profiles of Figure S4.

5. Pyridine Adsorption in liquid phase

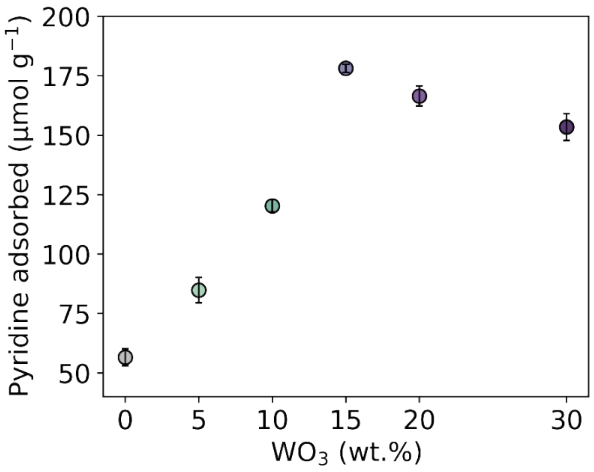

Figure S6. Calculated adsorbed pyridine for the for the WO_3/TiO_2 catalysts.